Applied Physics A (2026) 132:279
https://doi.org/10.1007/s00339-026-09485-3

Applied Physics A
Materials Science & Processing

Modular enzymatic biosensor based on electrolyte-gated organic field-effect transistor for glucose and urea sensing

H. J. N. P. D. Mello[1,3] · S. Dalgleish[1] · G. Ligorio[1,2] · M. Mulato[4] · E. J. W. List-Kratochvil[1,2,5]

Received: 28 October 2025 / Accepted: 3 March 2026 / Published online: 13 March 2026

Abstract
Electrolyte-gated organic field-effect transistors (EGOFETs) have the potential to be versatile transducing devices for the realization of modular environmental monitoring and biomedical diagnostic sensor platforms. For the practical realisation the EGOFET offers several operation modes to transduce a specific analyte/receptor interaction into an easy to read out electrical response. Here we report on the interaction between the analyte (glucose and urea) using specific enzyme (glucose-oxidase and urease, respectively) based bioreceptor anchored to the EGOFET gate electrode rather than a binding/affinity device. The presented EGOFET-based enzymatic biosensor for glucose and urea displays a linear and analyte selective response in the range between 10^{-6} and 10^{-3} mol/L. Changes in the local ionic strength affect the Debye length which modulates the EGOFET responses through the electric double layer capacitance variation. The possibility of exchanging the modified gate electrode to detect specific analytes using the same EGOFET system allows the modular sensor which might be reused and applied for a broad range of applications.

Keywords EGOFET · Enzymatic biosensor · Electric double-layer capacitance · Debye length

1 Introduction

Aside from the main application of organic field-effect transistors (OFETs) in display and integrated circuit technologies, OFETs have proved to be excellent candidates as transducer devices for many different sensing applications [1–3]. The outstanding features of organic-based devices, such as low temperatures processability, low-cost fabrication, miniaturization and integration on flexible substrates, has led to smart (disposable) sensor assemblies for health-, food- and environmental monitoring [4–9]. Another attractive property of organic semiconductor (OSC) materials is the generally good biocompatibility, which is important when it comes to biomedical applications and the envisioned human interfacing [10–12]. Moreover, the chemical and physical properties of organic compounds can be tailored to obtain a distinct sensitivity and selectivity with respect to target analytes, or to meet a specific requirement [13–15].

For the emerging fields of biomedical diagnostics and environmental monitoring, sensing of ions and biological substances in appropriate aqueous media is of interest. Therefore, a water-stable operation of OFET-based sensors is crucial, demanding their operation at low voltages and the resistance of the semiconductor layer to degradation and/or delamination over extended operation under aqueous conditions. In general, low voltage operation can be achieved by employing gate insulators with a high capacitance (using thin high-k dielectrics [16] or electrolytes [17]). Especially, the electrolyte gated field-effect transistor (EGOFET) architecture, which differs from an OFET by having the gate separated from the transistor's channel by an electrolyte, has shown much promise [18–21]. The non-linear potential

✉ H. J. N. P. D. Mello
hugomello@ufg.br

[1] Institut für Physik, Institut für Chemie, Humboldt-Universität zu Berlin, Zum Großen Windkanal 2, 12489 Berlin, Germany

[2] Center for the Science of Materials Berlin, Zum Großen Windkanal 2, 12489 Berlin, Germany

[3] Institute of Physics, Federal University of Goiás, Goiânia 74001-970, GO, Brazil

[4] Department of Physics, Faculty of Philosophy, Sciences and Letters at Ribeirão Preto, University of São Paulo, Ribeirão Preto 14040-901, SP, Brazil

[5] Helmholtz-Zentrum Berlin für Materialien und Energie GmbH, Hahn-Meitner-Platz 1, 14109 Berlin, Germany

drop across the electrolyte, due to the formation of electric double layers (EDLs) at the gate/electrolyte and OSC/electrolyte interfaces, realizes high capacitance values for the gate dielectric, thereby allowing for low voltage operation (< 1 V) and high-density charge accumulation [22]. The charge distribution in an EDL can be described by the Gouy-Chapman-Stern model and the EDL capacitance can be related to the Debye length [23] according to:

$$C_{DL} = \frac{\epsilon_r \epsilon_0}{\lambda_D} \tag{1}$$

where C_{DL} represents the capacitance of the electrical double layer, λ_D is the Debye length, and the parameters ε_r and ε_0 are the relative and the vacuum permittivity, respectively. Thus, the expression for the channel current formula of EGOFET model can be expressed as [24]:

$$I_{DS} = \frac{W}{L} \cdot \mu \cdot C_{DL} \cdot \left[V_{GS} - V_{th} - \frac{V_{DS}}{2} \right] \cdot V_{DS} \tag{2}$$

Where W and L are channel width and length, respectively, μ is the charge mobility, C_{DL} is the capacitance of the device, V_{th} is the threshold voltage for the device, V_{GS} is the potential applied to the gate and V_{DS} is the electrical bias applied between drain and source electrodes. Therefore, the EGOFET platform is extremely sensitive to modifications at the gate electrode [25, 26] as well as the composition of the electrolyte. For sensing applications, the electrolyte in the EGOFET can act as an analyte medium where high sensitivity can be achieved as a result of analyte-induced changes to the electrochemical potential across the dielectric (see below for more detail) [27]. In order to achieve analyte selectivity, a receptor site can be incorporated into the device and several different sensing concepts based on EGOFETs have been demonstrated so far [28–36]. For operation under electrostatic control, i.e. where chemical/electrochemical doping of the channel are assumed absent, two concepts for achieving analyte selectivity have been developed, either based on functionalization of the semiconductor surface [37–39] or the gate electrode [40–42]. In the first sensing concept, the semiconductor itself serves as the transducer. Depending on the device, the active area may be restricted to the surface, where adsorption of analyte molecules modifies the local charge distribution and thereby the conductivity of the channel, or it may extend into the bulk, where analyte permeation or doping directly alters the carrier density throughout the material. In both cases, the semiconductor material and device must be tailored to the specific analyte, since the interaction mechanism is intrinsic to the semiconductor. In the second sensing concept, by contrast, the gate surface is functionalized with a receptor that selectively binds the analyte. This receptor–analyte interaction is then transduced capacitively into the channel, enabling a modular architecture in which the same semiconductor device can be combined with differently functionalized gates, each dedicated to a particular analyte.

In this study, we use the latter concept and we investigate enzymatic biosensors for the detection of glucose and urea using an EGOFET architecture where the gate electrode is selectively functionalized (Fig. 1 (a)) with glucose oxidase (GOx) or urease (Ur), respectively, via grafting using *N*-hydroxysuccinimide/1-ethyl-3-(3-dimethylaminopropyl) (NHS/EDC) chemistry onto 11-mercaptoundecanoic acid (MUA) modified gold wire gate electrodes [43, 44]. The active channel was formed from poly(3-hexylthiophene) (P3HT), which remained physically and chemically decoupled from the enzymatic reactions, and has previously shown very stable performance in EGOFET devices using aqueous electrolyte systems and operational gate voltages below 600 mV [45, 46]. This study brings an EGOFET biosensors

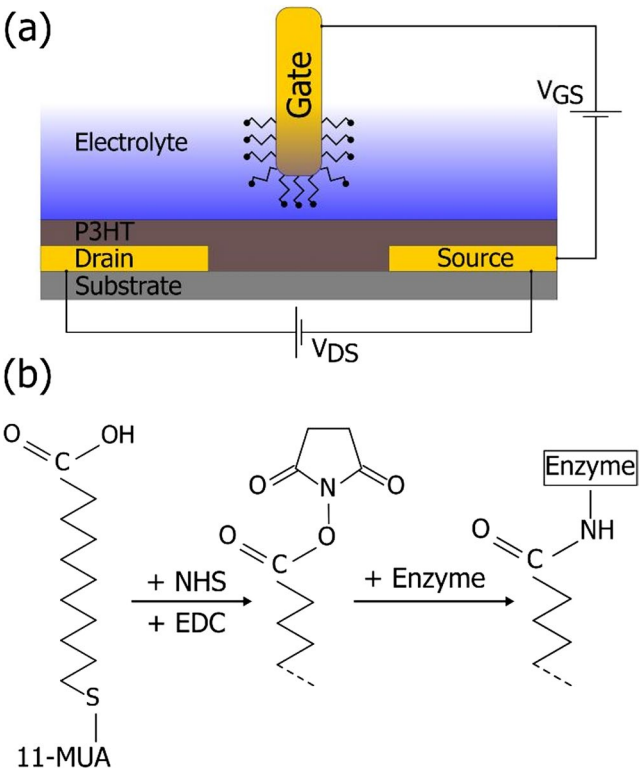

Fig. 1 The functionalization of the gate electrode of an EGOFET (showed in cross-section in **a**), allows for the fabrication of biosensor for analytes such as urea or glucose. In (**b**), from left to right the strategy for the enzyme immobilization onto carboxylate-terminated SAMs on Au gate rod is shown. Starting with MUA-SAM linker, followed by the addition of NHS and the water soluble carbodiimide EDC to the SAMs results in the formation of an NHS ester. Reaction of enzyme side-chain lysine residues with the ester results in the formation of an amide bond

based on enzymatic reactions which have been widely exploited in OECT [47, 48] (organic electrochemical transistor) based devices while EGOFETs are based on binding/affinity reactions [49]. The EGOFET allows the reuse of the sensor, not the case for OECTs due to ion penetration from electrochemical reactions and doping to the OSC layer and presents an architecture appropriate for biosensing applications. We evaluate the transduction physics of the EGOFET developed, which operates through the electric double layer capacitance variation rather than interfacial electrochemical processes in the gate/electrolyte interface, enabling sensor reuse and providing a modular biosensing strategy. From a broader perspective, the development of low-voltage, solution-processable transistor architectures such as EGOFETs aligns with international roadmaps for emerging electronic technologies, which emphasize flexible, energy-efficient, and application-specific devices. Modular biosensing platforms based on EGOFETs represent a promising route toward scalable and reconfigurable bioelectronic systems.

2 Materials and methods

2.1 Device fabrication

The EGOFET devices were fabricated using low-density prefabricated OFET test chips (Ossila Ltd, Sheffield, UK) comprising a Si^{++}/SiO_2 (d_{ox} = 300 nm) substrate structured with gold source, drain and gate electrodes (channel length $L = 30$ µm and channel width $W = 1$ mm) having prefabricated octadecyltrichlorosilane/2,3,4,5,6-pentafluorobenzenethiol (OTS/PFBT) layers on the SiO_2/Au surfaces, respectively. The substrates were cleaned by sonication method for five minutes in deionized (DI) water and acetone. After drying under a flow of N_2, the substrate was used immediately. Regioregular poly(3-hexylthiophene) (P3HT) (Rieke Metals, Lincoln, Nebraska, USA, MW = 37,000 g/mol, 98% regioregular) was deposited from a 5 mg/mL chlorobenzene solution. All devices were deposited via spin-coating (1000 rpm, for 60 s) and annealed on a hot plate for 30 min at 120 °C, inside a N_2 glovebox.

2.2 Gate functionalization

The EGOFETs were gated via a gold (Au) functionalized electrode. The gate wire functionalization occurred via enzyme immobilization on the wire's structure, as shown on Fig. 1 (b). The Au gate wire (approximately 25 mm length and 1.0 mm diameter) was immersed on a 11-Mercaptoundecanoic acid (MUA) ethanol solution (10 mmol/L) for 20 h to ensure the formation of a dense and well-ordered monolayer [50]. The MUA was used to form a self-assembled monolayer (SAM) on the gold gate electrode through thiol–gold chemisorption, providing terminal carboxyl groups for subsequent covalent enzyme attachment. Upon removal from the solution, the sample was rinsed twice with absolute ethanol and dried in a nitrogen stream. Next, the Au gate wire was immersed in a 0.05 mol/L N-hydroxysuccinimide (NHS) and 0.20 mol/L 1-ethyl-3-(3-dimethylaminopropyl (EDC) DI-water solution for 1.5 h [51]. The solution was prepared immediately before use. Activation with NHS/EDC enables the formation of reactive esters, which react with lysine residues of the enzymes to form stable amide bonds. Upon removal from the solution, the sample was rinsed with DI-Water. Finally, the Au gate wire was immersed in a 10 mg/mL enzyme solution (GOx or Ur) in phosphate buffer solution (PBS) for 1.5 h [52]. Upon removal from the solution, the sample was rinsed with PBS and stored under dry condition at 4 °C in a refrigerator when not in use. All experiments were carried out at room temperature.

2.3 Biosensor testing

A reservoir, made of polydimethylsiloxane (PDMS, Sylgard 184) was used to confine the static electrolyte, which was either deionized water, or an aqueous solution of glucose or urea. PDMS was chosen for its ease of fabrication and chemical compatibility with aqueous electrolytes. The devices were completed by inserting the (modified) gate electrode into the electrolyte solution. Electrical characterization was performed in air with the device connected to a dual channel Keithley 2636B SMU controlled via a home-written LabVIEW program, measuring the output and transfer characteristics of the devices in V_{GS} and V_{DS} ranges over which such devices have been shown to operate stably [53].

Solution exchange of the reservoir was performed manually using two syringes, one for introducing the new electrolyte to be measured and another for removing the existing solution already measured, in a home-made fluid circuit. This configuration ensured that the P3HT channel was continuously immersed in the electrolyte and never exposed to air during the experiments. During electrical measurements, the electrolyte remained static, and no continuous flow was applied. The volume of flushed electrolyte was 5 mL for every exchange. Figure SM 1 in the Supporting Information shows a schematic and a photograph of the experimental setup.

3 Results and discussion

3.1 Sensing mechanism

Regarding the enzymatic biosensors, the interactions between analytes and the enzyme for FET based devices

produce species which results in electronic perturbations in the system generating an output. Generally, the enzymes are immobilized on one of both interfaces gate electrode/electrolyte or electrolyte/OSC. Upon a binding event between the substrate and the enzyme, the products of the reactions contribute to the transduction process. The reaction mechanism for glucose start with its catalysis to gluconic acid and hydrogen peroxide, followed by the latter's oxidation leading to oxygen and proton ions at the appropriate potential (0.75 V) [54], while the reaction mechanism for urea is described by its hydrolysis catalysis to ammonium, hydroxyl ion and bicarbonate ions [55]. Both processes are shown below:

$$\begin{aligned} &\text{Glucose} + O_2 \xrightarrow{\text{Glucose oxidase}} \text{gluconic acid} + H_2O_2 \\ &\text{Urea} + 3 \cdot H_2O \xrightarrow{\text{Urease}} HCO_3^- + 2 \cdot NH_4^+ + OH^- \end{aligned} \quad (3)$$

Figure 1 (a) depicts the schematic of a device with a functionalized gate electrode for biosensor applications, showing the cross-section of the EGOFET device with a P3HT layer over the drain and source contacts, on top of the substrate. The (modified) gate electrode is dipped in the electrolyte to complete the device structure. For gate electrodes modified according to the reaction scheme in Fig. 1 (b), the enzymatic recognition/conversion of the analyte is able to cause a combined effect on the device, a local change to the electrochemical potential at device interfaces and changes in the transconductance of the EGOFET which, in turn, affects the charge accumulation in the P3HT channel, thereby yielding a detectable current response [41]. It is important to note that hydrophobic interactions at PDMS interfaces may influence biomolecular processes [56] and that alternative reservoir materials could be explored in future studies.

For field effect based biosensors the change in conductance is the principal reason for the potential difference variation measurable in EGOEFT devices [57]. As noted by Huang and co-workers, variations in conductance can arise from multiple mechanisms associated with chemical reactions and structural reorganization upon analyte–receptor binding, and device optimization is often guided by empirical approaches. The underlying mechanisms include orbital hybridization, surface polarization effects, changes in dipole moment, as well as adsorption and affinity binding of various biomolecules. Torsi and co-workers [58], demonstrated an example of electrical dipole formation due to binding of dopamine to a self-assembled monolayer of boronic acid. The interactions between analyte and enzyme produce electroactive species which results in electronic perturbations at the device interface. The products act modifying the system conductance by changing the enzyme/electrolyte capacitance. With increasing analyte concentration, the system capacitance also increases, along with the drain-source current.

3.2 EGOFET-based biosensor performance

In a first step, the EGOFET performance was studied with the bare Au gate electrode and the two modified Au gate electrodes: one functionalized with glucose-oxidase (GOx/Au), and the other with urease (Ur/Au), using DI water as the gate dielectric. Figure 2 (a) shows a comparison of the transfer curve in the linear regime from the three different gate electrodes (for the transfer curve in the saturation regime, see Supporting Information Figure SM 2). A shift in threshold voltage is observed with gate functionalization. For the bare-Au gate, the I_{DS} current reaches approximately 0.06 µA at V_{GS} = – 0.3 V in the linear regime (V_{DS} = – 0.1 V), while for the GOx and Ur modified gate, the I_{DS} results approximately 0.02 and 0.04 µA at V_{GS} = – 0.3 V, respectively. For both enzymatic modified gates, a shift in the threshold voltage occurred, varying from 0.23 ± 0.01 V for bare Au to 0.03 ± 0.01 and – 0.06 ± 0.01 V for GOx and Ur modified gate, respectively. The enzymatic functionalization of the gate's electrode give rise to a negative shift of threshold voltage which means that both enzymes reduce the charge carrier density in the organic channel with respect to bare Au electrode [59]. The threshold voltage is affected by the variation in the gate's surface potential [25] which is induced by the surface coverage of the Au electrodes with the enzymes [60].

To verify the device response to the analyte concentration, the transfer curves of the GOx-modified device were measured for different concentrations of glucose in DI-water. The concentration of glucose ranged from 10^{-6} to 10^{-1} mol/L. Figure 2 (b) shows the evolution of the GOx-modified EGOFET transfer curves (in the linear regime), when the measurement is carried out with increasing glucose concentration (from 10^{-6} to 10^{-3} mol/L, DI-water is also reported as reference). In the linear regime (V_{DS} = – 0.1 V, fixed in the V_{GS} = – 0.3 V) the outputted I_{DS} level for the glucose solution ranging from 10^{-6} to 10^{-3} mol/L changes from 0.025 µA to 0.040 µA. Equivalent results are obtained with the urea biosensor, using the Ur-modified gate (see Supporting Information Figure SM 3).

From the devices' transfer curve (measured in the linear regime), it is possible to obtain a calibration curve for the glucose biosensor. The calibration curve is shown in Fig. 3 (a) as relative variation of drain current ($\Delta I_{DS}/I_{DS}$ = (I_{DS} (solution) – I_{DS} (DI-water))/ I_{DS} (solution)) as a function of the glucose concentration (from 10^{-6} to 10^{-1} mol/L). As expected, the relative electrical response of the device using the bare-Au as gate is negligible (grey circles). (The transfer curves in linear regime for Au gate rod measuring

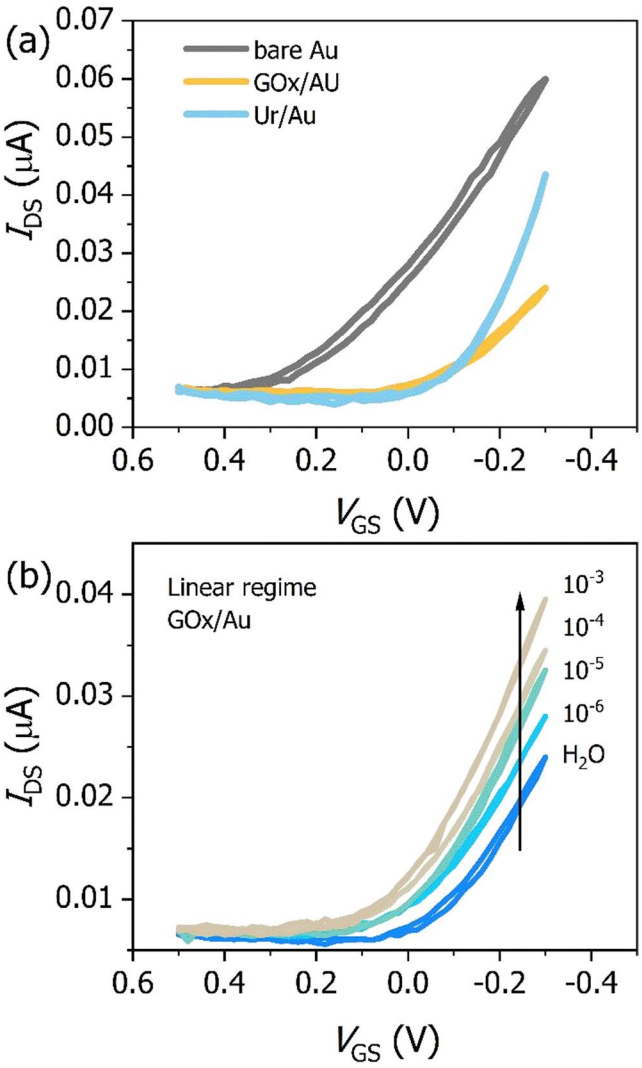

Fig. 2 Transfer curves of P3HT transistors in the linear regime with three different gate electrodes: The Au bare gate wire, the glucose-oxidase, GOx/Au, modified gate wire and the urease, Ur/Au, modified gate wire in (**a**). Variation in the transfer curve in the linear regime, V_{DS}=−0.1 V, for the glucose biosensor, GOx/Au, at glucose concentration varying from 10^{-6} to 10^{-3} mol/L and for DI-water

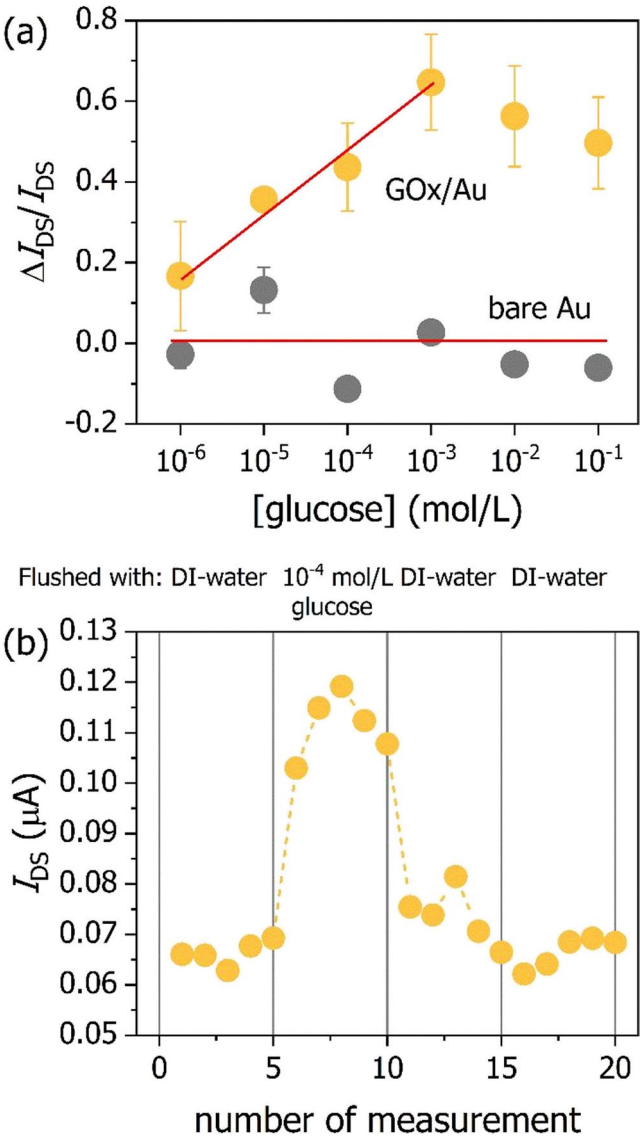

Fig. 3 In (**a**) the changing in the relative drain-source current ($\Delta I_{DS}/I_{DS}$) of the EGOFET device for the glucose biosensor, GOx/Au, at glucose concentration varying from 10^{-6} to 10^{-1} mol/L in the linear regime, V_{DS}=−0.1 V, in a forward measurement protocol. The same response for the EGOEFT device for the Au bare gate rods also shown. In (**b**) the reversibility analysis of the EGOFET based glucose biosensor. The first five experiments were done with pure water, then with glucose at 10^{-4} mol/L and back to pure water until the device recovered it previous response level

glucose and urea can be found in Supporting Information Figure SM 4). For the GOx-modified gate, the relative drain current change is linearly proportional to the logarithm of the glucose concentration between 10^{-6} and 10^{-3} mol/L, resulting in a limit of detection of $5.5 \pm 0.6 \times 10^{-6}$ mol/L and a limit of quantification of $18.3 \pm 2.1 \times 10^{-6}$ mol/L (using IUPAC definitions). For concentration higher than 10^{-3} mol/L the change in electrical response saturates. The drain-source current of the biosensor does not change accordingly to the analyte concentration, remaining at, approximately, 0.05 μA.

To investigate the device reversibility, the home-made fluid circuit was connected to the PDMS reservoir to be able to change the analyte concentration during the measurements via injection, while always keeping the gate immersed and the semiconductor layer covered with electrolyte. It has been reported that P3HT does not remain stable when exposed to oxygen. Especially when combined with light, Abdou et al. showed that it leads to an increase in carrier concentration and conductivity of the material, associated with a decrease in mobility by field effect, due to the presence of scattering centres of carriers [61]. The fluid circuit was necessary to yield reversibility since without it, the

devices underwent a rapid degradation [62] (The evolution of the relative drain current after a sequence of measurements with and without the fluid circuit can be found in Supporting Information Figure SM 5). First the measurements were carried out in DI-water, then following the injection of a 10^{-4} mol/L glucose solution, and finally the measurements were repeated once the solution was flushed with DI-water, and flushing was repeated until the current level returned to its original level. Five measurements were made for each change in electrolyte solution. Figure 3 (b) shows the results of this analysis for the GOx electrode system. The GOx/Au system presented a reversible operating mode. This result is important since it indicates that the system may be reused using differently functionalized gates for different analyte detection.

The same experimental procedures were performed to test the urea biosensor, i.e. the measurements were carried out with a P3HT based EGOFET device employing an Ur-modified gate and variable urea concentrated solutions. Figure 4 (a) shows the relative change in the drain-source current as function of the urea concentration. The measurements were first carried out with the bare-Au gate which yielded no response to changes in the urea concentration between 10^{-6} and 10^{-1} mol/L. As seen for the glucose biosensor, the drain current level increases linearly with the logarithm of the analyte concentration, and the saturation point is reached at 10^{-3} mol/L, resulting in a limit of detection of $7.2 \pm 1.1 \times 10^{-6}$ mol/L and a limit of quantification of $23.8 \pm 3.6 \times 10^{-6}$ mol/L (using IUPAC definitions). The reversibility of the urea biosensor was tested with the similar home-made setup used in the GOx-modified EGOFET described above. The device was first measured in DI-water and showed a consistent value of I_{DS} with time, as shown in Fig. 4 (b). Upon injection of the urea solution (10^{-4} mol/L) the device showed an abrupt increase in I_{DS}, demonstrating the immediate electrical response as result of the hydrolysis of urea by the enzyme. The reservoir was then flushed with several cycles of DI-water. Unlike for the glucose sensor, the decay in I_{DS} was much slower following the flushing of the urea. However, with repeated flushing, the device response showed a clear trend towards its original value. At higher concentrations the device is poorly reversible.

In an EGOFET-based biosensor, biorecognition events alter the conformation and/or charge distribution of the bioreceptors at the interfaces, thereby shifting the transistor's threshold voltage or altering transconductance [63, 64]. As previously described, enzymatic biosensors exhibit changes in the slope of the transfer curves indicating variations in the device's transconductance [65]. Figure 5 (a) shows the relative change in threshold voltage as a function of analyte concentration. The data show no variation in changes in analyte concentration between 10^{-6} and 10^{-1} mol/L. Not only

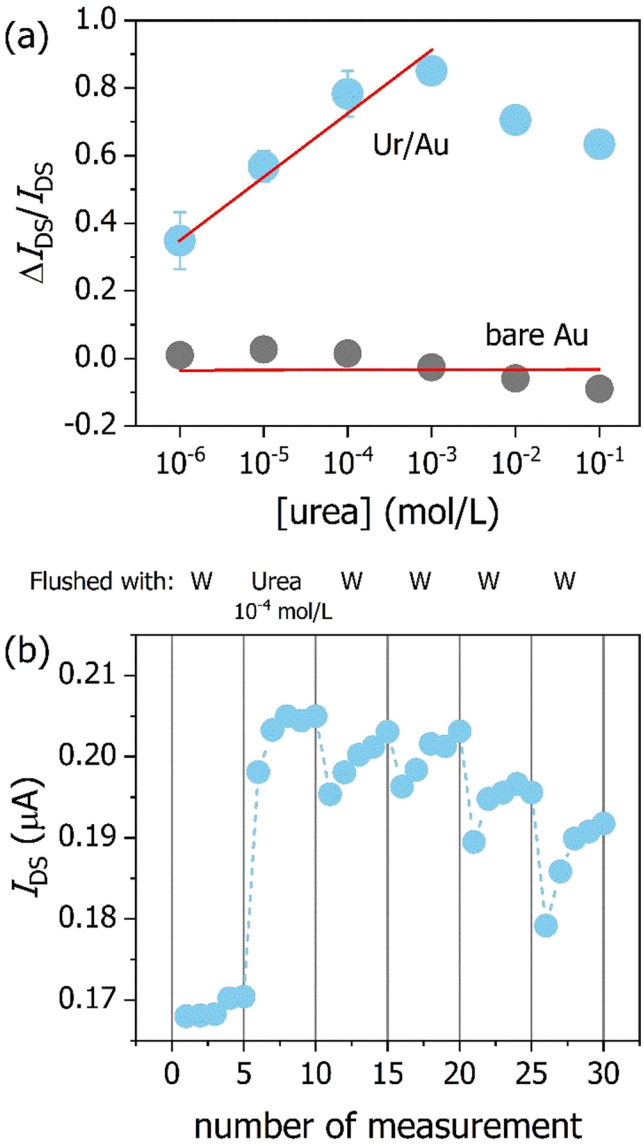

Fig. 4 In (**a**) the changing in the relative drain-source current ($\Delta I_{DS}/I_{DS}$) of the EGOFET device for the urea biosensor, Ur/Au, at glucose concentration varying from 10^{-6} to 10^{-1} mol/L in the linear regime, $V_{DS}=-0.1$ V, in a forward measurement protocol. The same response for the EGOEFT device for the Au bare gate is also shown. In (**b**) the reversibility analysis of the EGOFET based urea biosensor. The first five experiments were done with pure water, then with urea at 10^{-4} mol/L and back to pure water for 4 times

does the device operate below any redox potential for redox reactions involving the products of the enzymatic reaction [66], but direct electron transfer between the GOx enzyme and the Au electrode is also extremely difficult because the active site of GOx, (flavin adenine dinucleotide) FAD, is deeply embedded within a protective protein shell [67, 68].

Due to the isolation between the gate and channel regions in the EGOFET, local processes occurring at the gate/electrolyte interface do not influence channel properties [69].

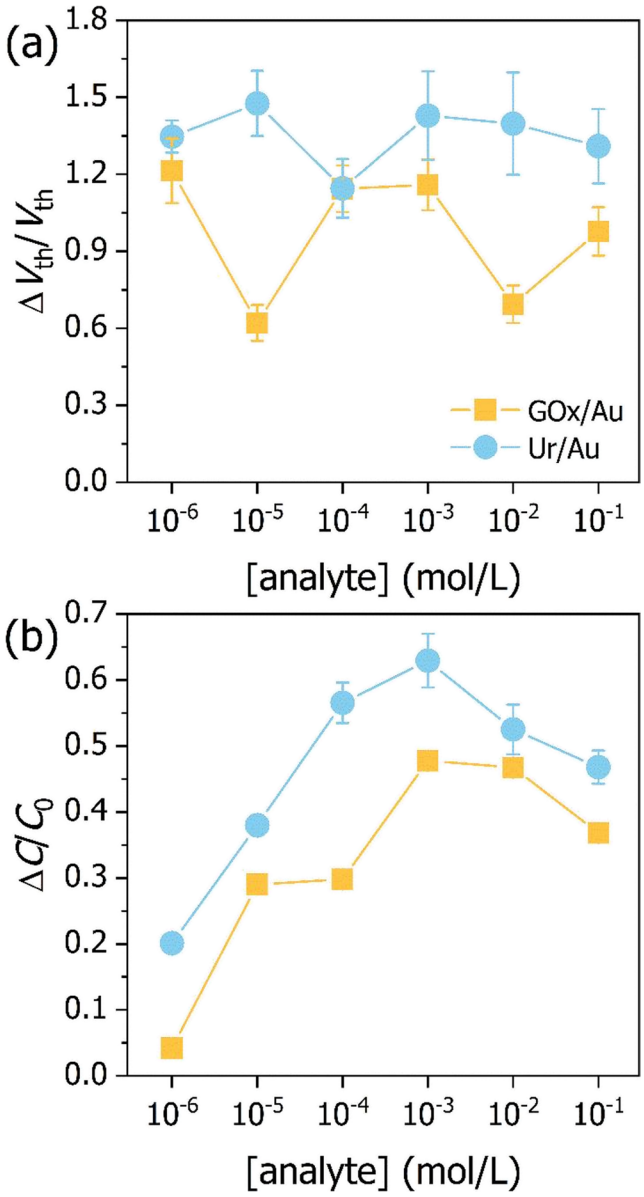

Fig. 5 In (**a**) the changing in the relative threshold voltage and in (**b**) the changing in the relative capacitance of the EGOFET device as function of both the analyte concentration, glucose and urea. There is no variation in relative threshold voltage to changes in both analytes' concentration while the relative capacitance shows variation in the same pattern of the calibration curves with relative drain-source current

Therefore, changes in transconductance are changes in capacitance, if channel mobility is kept constant:

$$g_m = \frac{W}{L} \cdot \mu \cdot C_{DL} \cdot V_{DS} \tag{4}$$

where g_m is the transconductance in the linear regime. Figure 5 (b) shows the relative change in capacitance as function of the analyte concentration. The variation in relative capacitance with change in analyte concentration between 10^{-6} and 10^{-1} mol/L follows the pattern presented in the calibration curves in Figs. 3 (a) and 4 (a) for glucose and urea measurements, respectively. This indicates that the EGOFET-based biosensor measures the change in capacitance of the EDL formed at the enzyme-modified gate electrode interface. This capacitance is smaller than the in series capacitance of the OSC/electrolyte (approximately 3–6 µF/cm^2) [45] and can be approximated as the total capacitance of the EGOFET. Changes in EDL capacitance are a consequence of variations in the Debye length (Eq. (1)) which are caused by local variations in ionic strength due to the release of products from reactions between enzymes and substrates [70–72]. The Debye length is inversely proportional to the square root of the ionic strength, according to [24]:

$$\lambda_D = \sqrt{\frac{\epsilon_r \epsilon_0 k_B T}{2 N_A e^2 I}} \tag{4}$$

where k_B is the Boltzmann constant, T is the temperature, N_A is the Avogadro constant, e is the elementary charge, and I is the ionic strength of the electrolyte.

The irreversibility of the devices at higher concentrations can be explained by local charge saturation at the enzyme-modified gate electrode interface. Nguyen and co-workers [60] demonstrated that the EDL capacitance saturates at specific analyte concentrations in EGOFETs with Au gate electrodes. At low concentrations, this process does not affect device sensitivity, but at higher concentrations of the target analytes, saturation is reached, affecting the EDL capacitance and influencing the biosensor response.

3.3 Biosensor selectivity

To test the enzymatic selectivity of the functionalized gate electrode, the relative drain-source current change ($\Delta I_{DS}/I_{DS}$) was calculated for the GOx-modified Au gate and the Ur-modified Au gate. First, the GOx/Au (Ur/Au) device was exposed to glucose (urea), followed by water, then urea (glucose), and finally to water (analytes concentration = 10^{-3} mol/L). Figure 6 displays the results of the measurements carried out with the functionalized gates as well as for a reference bare-Au gate. For the GOx-modified gate the glucose analyte gives a high response (approximately $\Delta I_{DS}/I_{DS} \sim 0.6$). However, in the presence of urea, the device also shows a modest increase in I_{DS} (approximately $\Delta I_{DS}/I_{DS} \sim 0.25$). Although the immobilization of GOx enzyme over substrates improved its stability, retaining its activity, the GOx denaturation by the presence of urea affect the enzymatic conformational structure, which induces interactions between the analyte and the bio-receptor [73]. In the case of the Ur-modified gate, the presence of urea showed a

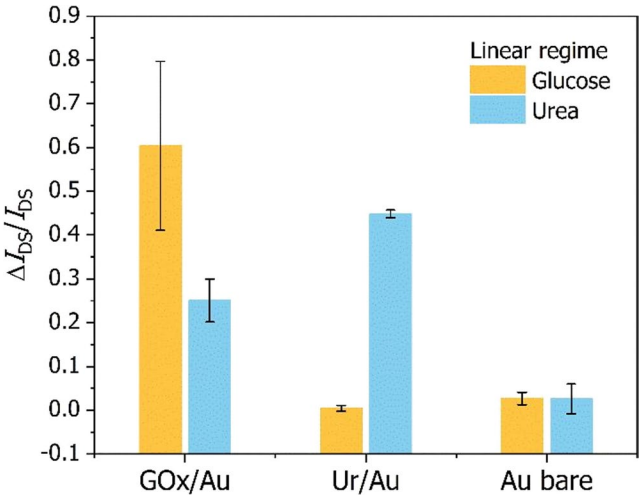

Fig. 6 Selectivity analysis of the EGOFET based enzyme modified biosensors with relative drain-source ($\Delta I_{DS}/I_{DS}$) of the device against glucose and urea analytes. The Au bare gate rod electrode was measured for non-specific binding analysis

high response (approximately $\Delta I_{DS}/I_{DS} \sim 0.45$), but showed negligible change in the presence of the glucose analyte (approximately $\Delta I_{DS}/I_{DS} \sim 0.0$). These results clearly show that both the proposed biosensors are selective regarding cross analysis between glucose and urea, with the Ur-modified gate showing almost perfect selectivity between these two analytes. In contrast, the bare Au gate showed negligible change in I_{DS} in the presence of either urea or glucose, showing that the specificity of the biosensor came from the enzyme immobilized in the gate electrode.

4 Conclusions

From the presented results it is possible to summarize that the coating of the enzymes in the Au gate rod was successfully achieved, and thus enzymatic biosensors based on P3HT EGOFET devices were realized. A change in analyte concentration induces a variation in the EGOFET response through modulation of the electric double layer capacitance, which arises from changes in the local ionic strength and the associated variation of the Debye length. For both biosensors the linear range was from 10^{-6} to 10^{-3} mol/L, after which, a saturation in the response was observed in both cases. To be a useful biosensor device, reversibility should be observed, as was demonstrated for measurements with a 10^{-4} mol/L solution. It is noteworthy that this system follows a modular design, allowing the functionalized gate to be exchanged without compromising the performance of the EGOFET, provided that the active channel remains intact and is not subjected to chemical or electrochemical doping. In this study, devices were investigated with GOx-modified Au and Ur-modified Au gate electrodes. The devices also exhibited cross-selectivity toward their respective target analytes, a crucial feature for applications in combined or matrix systems. Although the present study was carried out in controlled electrolyte solutions to understand the transduction mechanism of enzymatic EGOFET biosensors, the system is extendable to real biological samples and will be the subject of future work.

Supplementary Information The online version contains supplementary material available at https://doi.org/10.1007/s00339-026-09485-3.

Acknowledgements For financial support, Brazilian agencies are acknowledged. In addition, we would like to thank Prof. Louisa Reissig (Freie Universität Berlin) for providing customized LabVIEW programs for the FET measurements performed. This work was conducted within the framework of the Joint Lab GEN_FAB and benefited from the support of the HySPRINT Innovation Lab at Helmholtz-Zentrum Berlin. The authors also acknowledge the support of the Open Access Publication Fund of Humboldt-Universität zu Berlin.

Author contributions Hugo Mello: Conceptualization, Formal Analysis, Methodology, Investigation, Writing – Original draft, Writing – review & editing. Simon Dalgleish: Methodology, Investigation, Software, Supervision, Writing – Original draft. Giovani Ligorio: Methodology, Investigation, Software, Supervision, Writing – Original draft, Writing – review & editing. Marcelo Mulato: Funding acquisition, Supervision, Writing – review & editing. Emil List-Kratochvil: Resources, Funding acquisition, Methodology, Project administration, Supervision, Writing – Original draft, Writing – review & editing.

Funding The Article Processing Charge (APC) for the publication of this research was funded by the Coordenação de Aperfeiçoamento de Pessoal de Nível Superior - Brasil (CAPES) (ROR identifier: 00x0ma614). This research was funded by Fundação de Amparo à Pesquisa do Estado de São Paulo (FAPESP), with the following grant number 2014/09562-4, 2014/24559-0 and 2016/23305-0 and Conselho Nacional de Desenvolvimento Científico e Tecnológico (CNPq), with the following grant number 305380/2015-0, 310405/2021-1 and 303724/2025-0.

Data availability The data presented in this study are available on request from the corresponding author.

Declarations

Conflict of interest The authors declare no conflict of interest. The funders had no role in the design of the study; in the collection, analyses, or interpretation of data; in the writing of the manuscript; or in the decision to publish the results.

References

1. G. Horowitz, Adv. Mater. **10**, 365 (1998)
2. G. Horowitz, J. Mater. Res. **19**, 1946 (2004)
3. H. Sirringhaus, Adv. Mater. **26**, 1319 (2014)
4. S. Lai, F. Viola, P. Cosseddu, A. Bonfiglio, S. Lai, F.A. Viola, P. Cosseddu, A. Bonfiglio, Sensors. **18**, 688 (2018)
5. O. Knopfmacher, M.L. Hammock, A.L. Appleton, G. Schwartz, J. Mei, T. Lei, J. Pei, Z. Bao, Nat. Commun. **5**, 2954 (2014)
6. S. Hannah, A. Davidson, I. Glesk, D. Uttamchandani, R. Dahiya, H. Gleskova, Org. Electron. **56**, 170 (2018)
7. H.J.N.P.D. Mello, T. Heimfarth, M. Mulato, Mater. Chem. Phys. **160**, 257 (2015)
8. H.J.N.P.D. Mello, M. Mulato, Thin Solid Films. **656**, 14 (2018)
9. H.J.N.P.D. Mello, M. Mulato, Synth. Met. **239**, 66 (2018)
10. J.T. Mabeck, G.G. Malliaras, Anal. Bioanal Chem. **384**, 343 (2006)
11. J. Rivnay, R.M. Owens, G.G. Malliaras, Chem. Mater. **26**, 679 (2014)
12. M. Berggren, A. Richter-Dahlfors, Adv. Mater. **19**, 3201 (2007)
13. K. Schmoltner, F. Schlütter, M. Kivala, M. Baumgarten, S. Winkler, R. Trattnig, N. Koch, A. Klug, E.J.W. List, K. Müllen, Polym. Chem. **4**, 5337 (2013)
14. J. Kofler, K. Schmoltner, E.J.W. List-Kratochvil, in Proc. of SPIE. pp. 91851U-91851U–12 (2014)
15. A. Klug, M. Denk, T. Bauer, M. Sandholzer, U. Scherf, C. Slugovc, E.J.W. List, Org. Electron. **14**, 500 (2013)
16. H. Klauk, U. Zschieschang, J. Pflaum, M. Halik, Nature. **445**, 745 (2007)
17. M.J. Panzer, C.D. Frisbie, Adv. Mater. **20**, 3177 (2008)
18. L. Kergoat, B. Piro, M. Berggren, G. Horowitz, M.-C. Pham, Anal. Bioanal Chem. **402**, 1813 (2012)
19. F. Buth, A. Donner, M. Sachsenhauser, M. Stutzmann, J.A. Garrido, Adv. Mater. **24**, 4511 (2012)
20. A. Kyndiah, F. Leonardi, C. Tarantino, T. Cramer, R. Millan-Solsona, E. Garreta, N. Montserrat, M. Mas-Torrent, G. Gomila, Biosens. Bioelectron. **150**, 111844 (2020)
21. N. Lago, A. Galli, S. Tonello, S. Ruiz-Molina, S. Marino, S. Casalini, M. Buonomo, S. Pisu, M. Mas-Torrent, G. Giorgi, M.G. Pedersen, M. Bortolozzi, A. Cester, Adv. Electron. Mater. **11**, 2400134 (2025)
22. H. Du, X. Lin, Z. Xu, D. Chu, J. Mater. Sci. **50**, 5641 (2015)
23. R.E.G. van Hal, J.C.T. Eijkel, P. Bergveld, Sens. Actuators B **24**, 201 (1995)
24. K. Melzer, M. Brändlein, B. Popescu, D. Popescu, P. Lugli, G. Scarpa, Faraday Discuss. **174**, 399 (2014)
25. L. Kergoat, L. Herlogsson, B. Piro, M.C. Pham, G. Horowitz, X. Crispin, M. Berggren, PNAS. **109**, 8394 (2012)
26. S. Fabiano, S. Braun, M. Fahlman, X. Crispin, M. Berggren, Adv. Funct. Mater. **24**, 695 (2014)
27. D. Wang, V. Noël, B. Piro, Electronics. **5**, 9 (2016)
28. T. Cramer, A. Campana, F. Leonardi, S. Casalini, A. Kyndiah, M. Murgia, F. Biscarini, J. Mater. Chem. B **1**, 3728 (2013)
29. D. Berto Marcello, D.A. Chiara, P. Roberta, B. Marcello, Elena, Lauro Michele Di, Casalini Stefano, Cossarizza Andrea, Berggren Magnus, Simon Daniel, Spoto Giuseppe, Biscarini Fabio, and Bortolotti Carlo A. Adv. Biosystems. **2**, 1700072 (2017)
30. K. Schmoltner, J. Kofler, A. Klug, E.J.W. List-Kratochvil, Adv. Mater. **25**, 6895 (2013)
31. M. Magliulo, A. Mallardi, M.Y. Mulla, S. Cotrone, B.R. Pistillo, P. Favia, I. Vikholm-Lundin, G. Palazzo, L. Torsi, Adv. Mater. **25**, 2090 (2013)
32. K. Schmoltner, J. Kofler, A. Klug, and E. J. W. List-Kratochvil, in Proc. of SPIE. pp. 88311 N-88311 N–12 (2013)
33. C. Liao, M. Zhang, L. Niu, Z. Zheng, F. Yan, J. Mater. Chem. B **1**, 3820 (2013)
34. P. Lin, F. Yan, Adv. Mater. **24**, 34 (2012)
35. S. Ruiz-Molina, C. Martinez-Domingo, S. Ricci, S. Casalini, M. Mas-Torrent, ACS Appl. Electron. Mater. **6**, 8998 (2024)
36. G. Liang, L. Yang, L. Xiao, L. Tang, S. Cheng, Z. Sun, Y. Zhang, F. Yang, G.-J. Zhang, Biosens. Bioelectron. **286**, 117643 (2025)
37. J. Liu, M. Agarwal, K. Varahramyan, Sens. Actuators B **135**, 195 (2008)
38. L. Kergoat, B. Piro, M. Berggren, M.-C. Pham, A. Yassar, G. Horowitz, Org. Electron. **13**, 1 (2012)
39. I. Sergi, M. Sensi, R. Zanotti, T. Tsironi, E. Flemetakis, D.M. Power, C.A. Bortolotti, F. Biscarini, Biosens. Bioelectron. **271**, 117098 (2025)
40. K. Manoli, M. Magliulo, M.Y. Mulla, M. Singh, L. Sabbatini, G. Palazzo, L. Torsi, Angew. Chem. Int. Ed. **54**, 12562 (2015)
41. S. Casalini, F. Leonardi, T. Cramer, F. Biscarini, Org. Electron. **14**, 156 (2013)
42. G.D. Saygin, P. Greco, M. Selvaraj, M. Di Lauro, M. Murgia, M. Bianchi, L. Fadiga, F. Biscarini, Sens. Actuators B **404**, 135185 (2024)
43. J.J. Gooding, V.G. Praig, E.A.H. Hall, Anal. Chem. **70**, 2396 (1998)
44. M. Delvaux, S. Demoustier-Champagne, Biosens. Bioelectron. **18**, 943 (2003)
45. L. Kergoat, L. Herlogsson, D. Braga, B. Piro, M.-C. Pham, X. Crispin, M. Berggren, G. Horowitz, Adv. Mater. **22**, 2565 (2010)
46. D. Elkington, M. Wasson, W. Belcher, P.C. Dastoor, X. Zhou, Appl. Phys. Lett. **106**, 263301 (2015)
47. M. Montero-Jimenez, J.R. Neyra Recky, C. von Bilderling, J. Scotto, O. Azzaroni, W.A. Marmisollé, J. Electroanal. Chem. **978**, 118867 (2025)
48. M. Montero-Jimenez, J.R.N. Recky, O. Azzaroni, J. Scotto, W.A. Marmisollé, Chemosensors. **14** (2026)
49. S. Ricci, S. Casalini, V. Parkula, M. Selvaraj, G.D. Saygin, P. Greco, F. Biscarini, and M. Mas-Torrent, Biosensors and Bioelectronics. **167**, 112433 (2020)
50. N. Patel, M.C. Davies, M. Hartshorne, R.J. Heaton, C.J. Roberts, S.J.B. Tendler, P.M. Williams, Langmuir. **13**, 6485 (1997)
51. Q.-Z. Hu, C.-H. Jang, Colloids Surf., B **88**, 622 (2011)
52. X. Yang, L. Hua, H. Gong, S.N. Tan, Anal. Chim. Acta. **478**, 67 (2003)
53. H.J.N.P.D. Mello, S. Dalgleish, G. Ligorio, M. Mulato, List-Kratochvil, in *Organic and Hybrid Sensors and Bioelectronics XI*, ed. by I. Kymissis, R. Shinar, L. Torsi, E.J.W. List-Kratochvil (International Society for Optics and Photonics, 2018), p. 1073819
54. X. Feng, H. Cheng, Y. Pan, H. Zheng, Biosens. Bioelectron. **70**, 411 (2015)
55. B. Lakard, D. Magnin, O. Deschaume, G. Vanlancker, K. Glinel, S. Demoustier-Champagne, B. Nysten, A.M. Jonas, P. Bertrand, S. Yunus, Biosens. Bioelectron. **26**, 4139 (2011)
56. M.W. Toepke, D.J. Beebe, Lab. Chip. **6**, 1484 (2006)
57. W. Huang, A.K. Diallo, J.L. Dailey, K. Besar, H.E. Katz, J. Mater. Chem. C **3**, 6445 (2015)
58. L. Torsi, M. Magliulo, K. Manoli, G. Palazzo, Chem. Soc. Rev. **42**, 8612 (2013)
59. S. Casalini, A.C. Dumitru, F. Leonardi, C.A. Bortolotti, E.T. Herruzo, A. Campana, R.F. de Oliveira, T. Cramer, R. Garcia, F. Biscarini, ACS Nano. **9**, 5051 (2015)
60. T.T.K. Nguyen, H.V. Tran, T.T. Vu, S. Reisberg, V. Noël, G. Mattana, M.C. Pham, B. Piro, Biosens. Bioelectron. **127**, 118 (2019)

61. M.S.A. Abdou, F.P. Orfino, Y. Son, S. Holdcroft, J. Am. Chem. Soc. **119**, 4518 (1997)
62. A. Klug, A. Meingast, G. Wurzinger, A. Blümel, K. Schmoltner, U. Scherf, E.J.W. List, in Proc. of SPIE. pp. 811809-811809-15 (2011)
63. G. Palazzo, D. De Tullio, M. Magliulo, A. Mallardi, F. Intranuovo, M.Y. Mulla, P. Favia, I. Vikholm-Lundin, L. Torsi, Adv. Mater. **27**, 911 (2015)
64. M.Y. Mulla, E. Tuccori, M. Magliulo, G. Lattanzi, G. Palazzo, K. Persaud, L. Torsi, Nat. Commun. **6**, 6010 (2015)
65. F. Buth, D. Kumar, M. Stutzmann, J.A. Garrido, Appl. Phys. Lett. **98**, 153302 (2011)
66. M. Kaisti, Biosens. Bioelectron. **98**, 437 (2017)
67. Y. Yu, Z. Chen, S. He, B. Zhang, X. Li, M. Yao, Biosens. Bioelectron. **52**, 147 (2014)
68. J.T. Holland, C. Lau, S. Brozik, P. Atanassov, S. Banta, J. Am. Chem. Soc. **133**, 19262 (2011)
69. N. Wang, A. Yang, Y. Fu, Y. Li, F. Yan, Acc. Chem. Res. **52**, 277 (2019)
70. T. Cramer, A. Kyndiah, M. Murgia, F. Leonardi, S. Casalini, F. Biscarini, Appl. Phys. Lett. **100**, 143302 (2012)
71. A. Béraud, M. Sauvage, C.M. Bazán, M. Tie, A. Bencherif, D. Bouilly, Analyst. **146**, 403 (2021)
72. J. Zou, H. Bai, L. Zhang, Y. Shen, C. Yang, W. Zhuang, J. Hu, Y. Yao, W. Walter, Hu, J. Mater. Chem. B **12**, 8523 (2024)
73. S. Rauf, A. Ihsan, K. Akhtar, M.A. Ghauri, M. Rahman, M.A. Anwar, A.M. Khalid, J. Biotechnol. **121**, 351 (2006)